Bulgarian Chemical Communications, Volume 52, Issue 4 (pp. 493-499) 2020 *DOI: 10.34049/bcc.52.4.5288*

Studies on FeP/TiO_2 catalysts in the ammoxidation of 2-methyl pyrazine to 2-cyano pyrazine

N. Pasupulety*, M. Daous, A. A. Al-Zahrani, H. Driss, L. A. Petrov

Chemical and Materials Engineering Department, Faculty of Engineering, King Abdulaziz University, P.O. Box 80204, Jeddah 21589, Saudi Arabia

Received: June 06, 2020; Revised: July 18, 2020

Nominal loadings of iron phosphate (FeP) from 5 to 25 wt% were deposited on TiO_2 (anatase) through a wet impregnation method. Vapor phase ammoxidation of 2-methyl pyrazine (2-MP) to 2-cyano pyrazine (2-CP) was carried out on these catalysts in the reaction temperature range of 633 to 693K at W/F= 2 g/(ml/h). Characterization of FeP/TiO_2 samples was done by using XRD, FTIR, laser Raman and potentiometric titration techniques. XRD analysis showed quartz type $FePO_4$ at 15 wt% of iron phosphate loading. Essentially, the quartz phase was intensified and new phases such as $TiPO_4$ and TiP_2O_7 were observed for 20 and 25FeP/TiO_2 samples. At lower FeP loadings (5 and 10 wt%) the quartz phase was inadequate and resulted in decreased ammoxidation activity. On the other hand, at higher FeP loadings (20 and 25 wt%) aggregation of $FePO_4$ and titanium phosphate phases reduced the ammoxidation activity. Among the catalysts studied, $15FeP/TiO_2$ showed 2-CP selectivity of 91% with 75.5% of 2-MP conversion at 653K. It is associated with (i) its higher acid strength and (ii) adequate active quartz phase dispersed on TiO_2.

Keywords: Iron phosphate; titanium dioxide; ammoxidation; 2-methylpyrazine; 2-cyano pyrazine

INTRODUCTION

Heterocyclic nitriles are valuable intermediates and reactants in the fine chemical sector. These nitriles are used for the synthesis of several pharmaceuticals, dyestuffs, pesticides, etc. [1, 2]. Alkyl heterocyclic compounds can be converted into their corresponding nitriles in a single step *via* ammoxidation process. Through this process one can achieve high yields of nitriles over direct vapor phase oxidation [3]. Essentially, V_2O_5 deposited on TiO_2, Nb_2O_5 and Al_2O_3 catalysts was investigated in the ammoxidation process [4-7]. The studies revealed that nitrile formation was influenced by the nature of support through metal-support interactions [8, 9]. However, usage of V_2O_5 supported catalysts in the ammoxidation process was limited by high temperature activity and over oxidation (led to undesired products). Further, vanadium phosphate deposited TiO_2 catalysts were investigated in the ammoxidation of 2,6-dichloro toluene [10]. Bulk lanthanum vanadate and iron phosphate catalysts were studied for 2-methyl pyrazine ammoxidation reaction [11-13]. However, these catalysts showed either lower selectivity or lower yield of 2-cyano pyrazine. In this regard, very few reports are available on supported iron phosphate catalysts for oxidation and ammoxidation reactions. McCormick *et al.* [14] have studied the methane oxidation process by employing iron phosphate deposited metal oxide (Al_2O_3, SiO_2, TiO_2 and ZrO_2) catalysts.

In the present study, the catalytic behavior of FeP/TiO_2 catalysts was investigated in the ammoxidation of 2-MP in the temperature range of 633-693K with W/F=2 g/(ml/h). The detailed catalyst characterization was carried out by using XRD, FTIR, FT-Raman and potentiometric titration techniques. The possible structure-activity correlations will be discussed further. To the best of our knowledge, this is the first report on FeP/TiO_2 catalysts for the vapor phase ammoxidation of 2-MP to 2-CP.

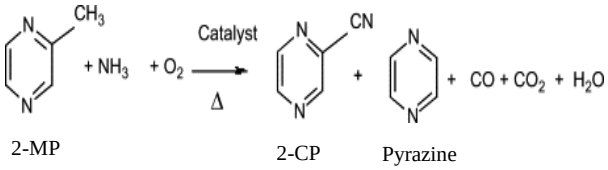

Scheme 1. Generalized 2-methyl pyrazine ammoxidation scheme.

EXPERIMENTAL

Catalyst preparation

Nominal loadings of iron phosphate (5 to 25 wt%) were deposited on TiO_2 (anatase, ≥ 99.8%, Sigma-Aldrich) by using a wet impregnation method. For example, 1.071 g of iron nitrate ($Fe(NO_3)_3.9H_2O$, ≥ 98%, Sigma-Aldrich) and 0.381 g of ammonium dihydrogen phosphate ($(NH_4)H_2PO_4$, Sigma-Aldrich) were used for 10 g of $5FeP/TiO_2$ catalyst with P-to-Fe atomic ratio of 1.2.

* To whom all correspondence should be sent:
E-mail: nsampathra@kau.edu.sa

The precursor salts were dissolved each in 25 ml of deionized water. These solutions were mixed together under continuous stirring at room temperature. TiO_2 powder was added to the above mixed solution and aged for 1 h. The excess water from the resultant slurry was removed on a preheated hot plate at 383 K. The obtained solid crystals were dried for 12 h in a preheated oven at 393 K. Finally, the dried mass was calcined in an oven at 823 K for 4 h in static air. These catalysts were denoted as 5FeP/TiO_2 for 5 wt.% of iron phosphate loading and so on so forth. Furthermore, 15FeP/CeO_2 and 15FeP/ZrO_2 catalysts were also synthesized by a wet impregnation method and used for comparison studies.

Catalysts characterization studies

N_2-physisorption studies of calcined TiO_2 and FeP/TiO_2 samples were carried out using a Micromeritics (Auto Chem-2910) instrument at liquid nitrogen temperature (77 K).

Powder X-ray diffraction analysis of calcined TiO_2 and FeP/TiO_2 samples was performed using a Rigaku Miniflex diffractometer at Cu K_α radiation (λ =1.5405 Å). FTIR spectra of spent catalysts were recorded on a DIGILAB (USA) spectrometer at a resolution of 4 cm^{-1} by the KBr disc method.

Fourier transform laser Raman spectroscopic measurements were carried out using a Bruker RFS 100/S spectrometer equipped with Nd:YAG laser (1.064 μm) and InGaAs detector. A laser power of 50 mW was employed.

The acid strength of calcined TiO_2 and FeP/TiO_2 samples was measured by the potentiometric titration method [15]. Each, 50 mg of sample was suspended in acetonitrile and kept under continuous stirring for 3 h. The resultant suspension was titrated with 0.05 N n-butyl amine acetonitrile solution at a flow rate of 0.05 ml/min. The variation in the electrode potential (E, mV) was measured with a digital pH meter (Automatic titrator, Schott GmbH, Germany), having a standard calomel electrode. The potentiometric titration was performed with a glass electrode. The instrument was calibrated using standard buffer solutions.

Catalytic reaction

Ammoxidation of 2-MP was carried out in a fixed-bed glass reactor in the temperature range of 633 to 673 K. In a typical experimental procedure, about 4 g of each FeP/TiO_2 sample was loaded in the reactor in between two quartz plugs. The feed composition ratio employed in this reaction was about 2-MP/water/ammonia/air = 1/13/17/38. The 2-MP solution was fed into the reactor by using a Braun pump at a flow rate of 2 ml/h. After attaining the steady state for 30 min, at each reaction temperature, the liquid product was collected for 10 min. The collected liquid sample was analyzed by GC equipped with FID connected to SE-30 column. Pyrazine was the major byproduct in this reaction. The CO_x selectivity (TCD, Restek Plot Q column) was found to be about 2 to 5 % under the studied reaction conditions.

$$\%\ X_{2\text{-MP}} = \frac{(\text{Moles of 2-MP, } \mathbf{in} - \text{Moles of 2-MP, } \mathbf{out})}{\text{Moles of 2-MP, } \mathbf{in}} \times 100$$

$$\%\ S_i = \frac{\text{Moles of product } \textit{i} \textbf{ out}}{(\text{Moles of 2-MP, } \mathbf{in} - \text{Moles of 2-MP, } \mathbf{out})} \times 100$$

$$\%\ \text{Yield} = \frac{\text{Moles of product } \textit{i} \textbf{ out}}{\text{Moles of 2-MP, } \mathbf{in}} \times 100$$

RESULTS AND DISCUSSION

N_2-physisorption studies

BET surface area results of TiO_2 and FeP/TiO_2 samples are presented in Table 1. Among the samples studied, TiO_2 showed the greatest surface area of 55 m^2/g. Deposition of FeP on TiO_2 decreased the BET surface area of the resultant sample. It is associated with the pore blockage of TiO_2 by FeP. Similar results were reported by McCormic *et al*. [13] for $FePO_4/Al_2O_3$ catalysts.

XRD analysis

Powder X-ray diffraction analysis results of FeP and FeP/TiO_2 samples are presented in Fig. 1. The bulk FeP primarily exhibited quartz type $FePO_4$ with a small amount of tridymite phase [16]. FeP/TiO_2 samples principally exhibited X-ray reflections related to TiO_2 anatase phase (ICDD

PDF 21-1272) up to 10 wt% of FeP loading. Essentially, X-ray reflections related to quartz type of $FePO_4$ phase was observed at 15 wt.% of FeP loading on TiO_2. After this loading, X-ray reflections of quartz type of $FePO_4$ was intensified and also new phases were observed for 20 and 25FeP/TiO_2 samples. X-ray reflections exhibited at 2θ = 20.2 and 25.8º correspond to quartz type of $FePO_4$ phase [16]. Further, the new X-ray reflections appeared at 2θ = 22.4, 34.8, 40.9, 54.6, 58.0, 71.0 and 78.2º correspond to crystalline $TiPO_4$ phase [ICDD No. 81-1334] and those at 28.6 and 67.6º correspond to TiP_2O_7 phase [ICDD No. 03-0300]. It is noteworthy that the titanium phosphate phases were not detected up to 15 wt% of FeP loading in FeP/TiO_2 samples. The formation of $TiPO_4$ and TiP_2O_7 phases in 20 and 25FeP/TiO_2 samples suggest that the stiochiometric excess of phosphate [17] interacts with TiO_2 during the calcination process. Glaum *et al*. [18] have reported that the $TiPO_4$ phase formation was due to the combination of TiO_2 and TiP_2O_7. McCormick *et al*. [13] pointed out that monolayer coverage of TiO_2 (anatase) can be achieved at 16 wt% of FeP loading. The XRD analysis results obtained in the present study are in agreement with the literature reports.

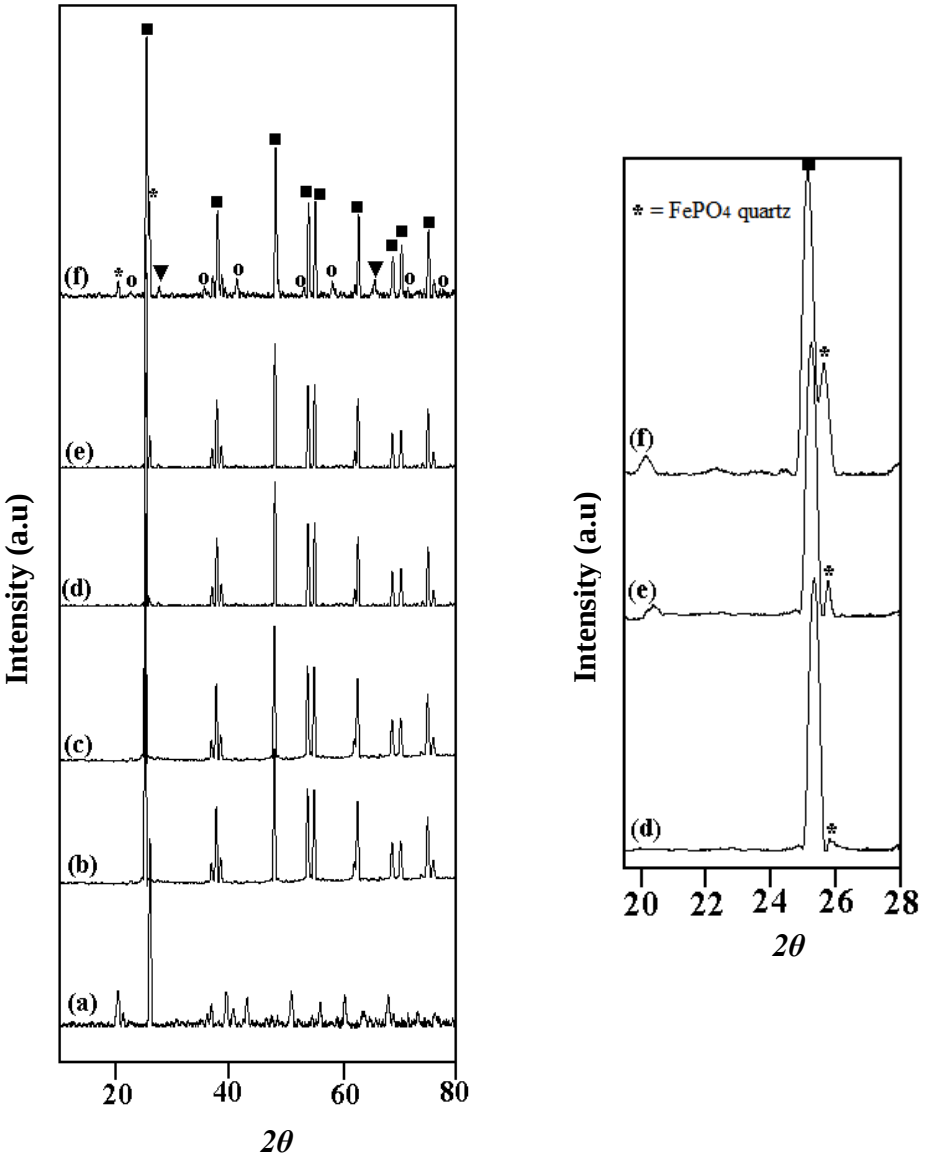

Fig. 1. XRD patterns of calcined iron phosphate catalysts supported on TiO_2. (a) Bulk FeP (b) 5FeP/TiO_2 (c) 10FeP/TiO_2 (d) 15FeP/TiO_2 (e) 20FeP/TiO_2 (f) 25FeP/ TiO_2 (∗) $FePO_4$ quartz phase (■) TiO_2 anatase (**o**) $TiPO_4$ (▼) TiP_2O_7

Laser Raman studies

FT-Raman spectral analysis results of TiO_2, FeP and FeP/TiO_2 samples are presented in Fig. 2. Bulk FeP exhibits the Raman vibrations in the region of 1000-1200 cm^{-1} due to the stretching and bending modes of phosphate groups [19]. Very strong Raman vibrations were observed for bulk TiO_2 in the region of 350-700 cm^{-1}. The Raman bands at 395, 510 and 635 cm^{-1} are assigned to the B1g, A1g and B2g modes of the TiO_2 anatase phase, respectively [20]. However, only TiO_2 vibrations were observed upbto 15 wt% of FeP loading on TiO_2. After this loading, the vibrations related to TiO_2 were reduced and new vibrations appeared at 280, 420, 1050 and 1180 cm^{-1} in the 20 and 25FeP/TiO_2 samples. The band appeared at 280 cm^{-1} is attributed to PO_4 tetrahedra units of $TiPO_4$ and the bands at 420 and 1180 cm^{-1} are characteristic bands for TiP_2O_7 [21]. The broad band appeared at 1050 cm^{-1} might be due to the asymmetric coupled vibration of phosphate groups of $FePO_4$. It is clear from the Raman data that titanium phosphate formation is taking place at higher loadings of FeP on TiO_2. These results are in good agreement with XRD data.

Acidity measurements by potentiometric titration

The potentiometric titration profiles of TiO_2 and FeP/TiO_2 samples are presented in Fig. 3 and the obtained acid strength values (E (mV)) are presented in Table 1. Linear butyl amine was used as a base component in the potentiometric titrations. Among the samples studied, pure TiO_2 showed lower acidity. A gradual increase in the acidity was observed upon a gradual increase in the FeP loading up to 15 wt% on TiO_2. After this loading, the acidity of the 20 and 25FeP/TiO_2 samples slightly decreased. It might be associated with the aggregated $FePO_4$ particles and/or surface phosphorus interaction with TiO_2 to form titanium phosphates. The decreasing order of acidity is as follows: 15FeP/TiO_2 > 20FeP/TiO_2 > 25FeP/TiO_2 >10FeP/TiO_2 > 5FeP/TiO_2 > TiO_2. At lower FeP loadings (5 and 10 wt%) the active $FePO_4$ phase was inadequate and resulted in lower acid strength.

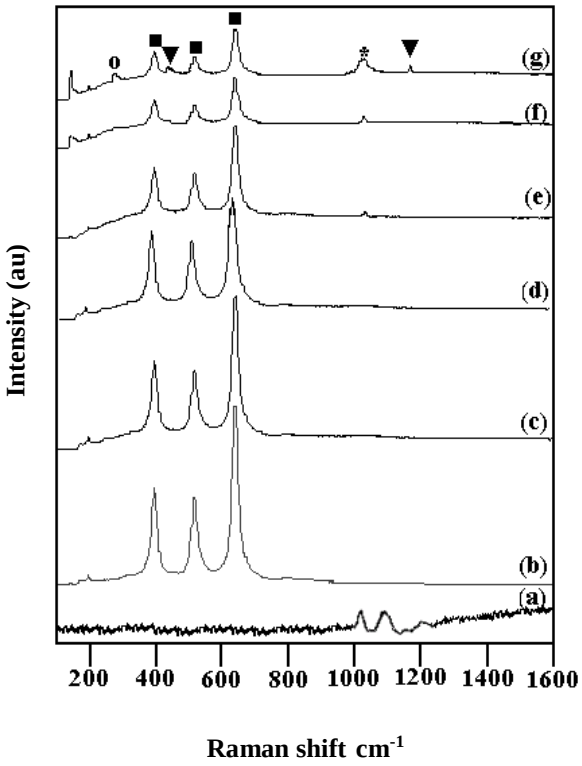

Fig. 2. FT-Raman spectra of calcined samples. (a) Bulk FeP (b) TiO_2 (c) 5FeP/TiO_2 (d) 10FeP/TiO_2 (e) 15FeP/TiO_2 (f) 20FeP/TiO_2 (g) 25FeP/TiO_2 (∗) $FePO_4$ (■) TiO_2 anatase (**o**) $TiPO_4$ (▼) TiP_2O_7

Table 1. BET surface area, SEM/EDX, acid strength and 2-CP selectivity results of TiO_2 and FeP/TiO_2 catalysts.

Catalyst	*SEM/EDX %	BET surface area (m^2/g)	Acid strength **E (mV)	(%) Selectivity 2-CP at 653 K
TiO_2 (anatase)	-	55	190	66
5FeP/TiO_2	4.65	45	340	71
10FeP/TiO_2	9.8	33	378	78
15FeP/TiO_2	14.5	21	438	91
20FeP/TiO_2	18.9	12	419	82
25FeP/TiO_2	24.6	8	390	75

* Analysis done using LEO-1530- Pegasus EDX system; ** Electrode potential values

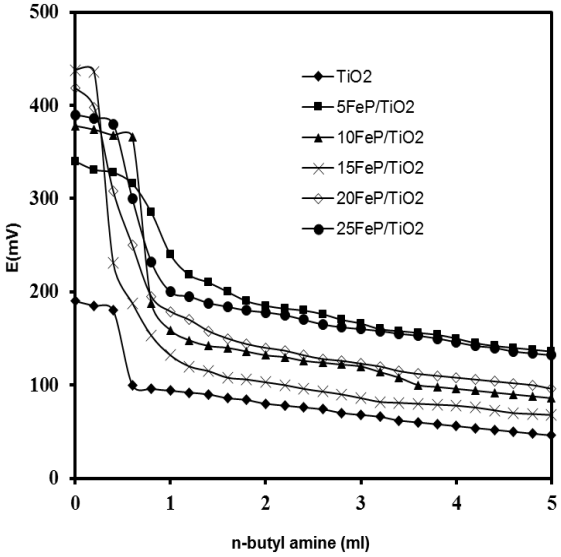

Fig. 3. Potentiometric titration curves of TiO_2 and FeP/TiO_2 catalysts.

Catalytic activity results

Catalytic activity results of TiO_2 and FeP/TiO_2 catalysts are shown in Fig. 4. Fig. 4(A) presents the conversion of 2-MP in the reaction temperature range of 633 to 693K. Among the studied catalysts, lowest conversion of 35% was obtained on pure TiO_2. The conversion of 2-MP increased with an increase in iron phosphate loading up to 15 wt% on TiO_2 and also increased with an increase in the reaction temperature from 633K to 693K. At 693K, about 80% of 2-MP conversion was obtained on the $15FeP/TiO_2$ catalyst. At higher loadings (20 and 25 wt%) the conversion of 2-MP leveled off under the studied reaction conditions. It is associated with titanium phosphate formation in 20 and $25FeP/TiO_2$ catalysts. These phosphates were active above 723 K in the ammoxidation of propylene to acrylonitrile [22]. Hence, titanium phosphates are either less active or high reactions temperatures are required for the ammoxidation of 2-MP. The order of 2-MP conversion at 693 K is as follows: $25FeP/TiO_2$ (81%) ≈ $20FeP/TiO_2$ (80%) ≈ $15FeP/TiO_2$ (79%) > $10FeP/TiO_2$ (68%) > $5FeP/TiO_2$ (60%) > TiO_2 (33%).

Fig. 4(B) presents the 2-CP selectivity results on TiO_2 and FeP/TiO_2 catalysts. Pyrazine (major byproduct) formation was found high at 673 and 693K. It might be associated with methyl group dissociation from 2-MP at higher reaction temperatures. On the other hand, higher 2-CP selectivity was found at lower reaction temperatures (633-653K). The maximum 2-CP selectivity of 92.5% was obtained on $15FeP/TiO_2$ at 633K. Further, the 2-CP selectivity decreased at higher FeP loadings (20 and 25 wt%). It is noteworthy that the acid strength increased up to 15 wt% of FeP loading and after this it slightly decreased. The results suggest that high acid strength was necessary for 2-CP formation during the ammoxidation reaction. In order to understand the influence of acid strength on 2-CP selectivity we examined the spent catalysts by FTIR technique and the resultant spectra are presented in Fig. 5A. The major band observed at 760 cm^{-1} is attributed to the Ti-O or Ti-O-Ti stretching vibration of TiO_2 in an octahedral coordination [23]. The band at 1040 cm^{-1} is ascribed to phosphate group vibrations of $FePO_4$ and $TiPO_4$ [24]. Further, the FTIR band observed at 565 cm^{-1} in 15, 20 and $25FeP/TiO_2$ is assigned to asymmetric stretching mode of the phosphate group of $FePO_4$. Apart from support and phosphate bands a new shoulder was observed at 1402 cm^{-1} in spent 15, 20 and $25FeP/TiO_2$ catalysts (for comparison purposes fresh FeP/TiO_2 FTIR spectra were added in Fig. 5B). It is associated with asymmetric stretching mode of ammonium ion of an ammonium complex of $FePO_4$ [19]. Further, it should be noted that the formation of ammonium complex is facile on catalysts with higher acid strength. Martin *et al*. [25] pointed out that the ammonium complex of the metal ion (V or Fe) can act as a source of N atoms to form the nitrile compound in the ammoxidation reaction. Hence, the observed high 2-CP selectivity on $15FeP/TiO_2$ is associated with its higher acid strength. Fig. 4(C) presents the major byproduct pyrazine formation on FeP/TiO_2 catalysts. About 29% of pyrazine formation was observed on support TiO_2 at 653K whereas pyrazine formation decreased with the increase in FeP loading on TiO_2. Only 7% of pyrazine formation was observed on $15FeP/TiO_2$. Further, pyrazine formation was improved on 20 and $25FeP/TiO_2$ catalysts.

It was reported that TiO_2 lattice oxygen participation in the thermally induced catalytic reaction of organic compounds results in the formation of a surface vacancy [28]. These defects in TiO_2 can improve the formation of pyrazine aldehyde intermediate from 2-MP and thereby influence the nitrile formation (2-CP).

CONCLUSIONS

Iron phosphate deposited TiO_2 (anatase) catalysts demonstrated good catalytic activity in the ammoxidation of 2-MP to 2-CP in the reaction temperature range of 633-693K. Essentially, at lower FeP loadings (5 & 10 wt%) the active $FePO_4$ phase was inadequate and resulted in low 2-MP conversion.

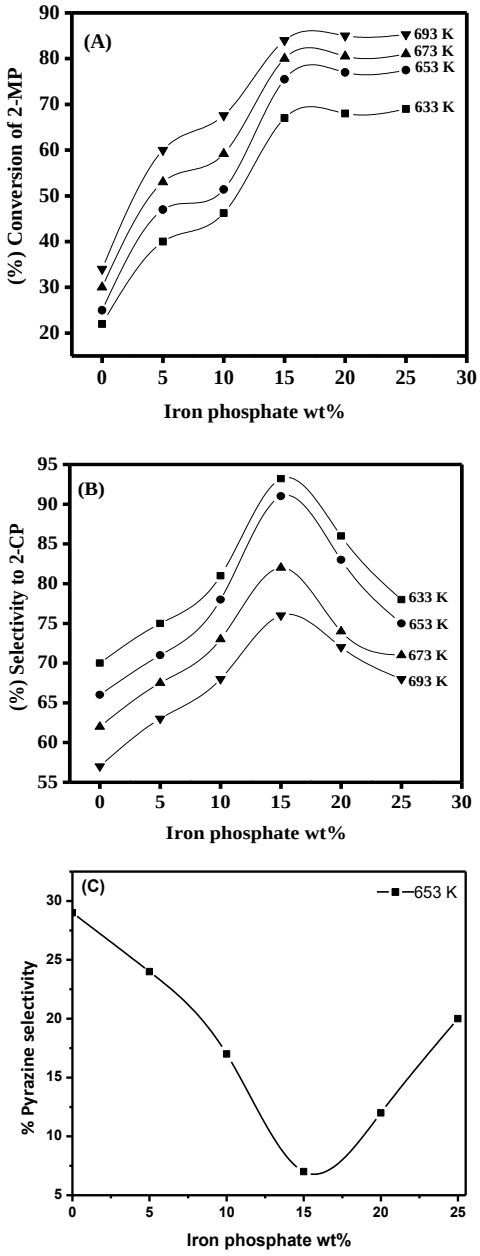

Fig. 4. (A) 2-MP conversion (B) 2-CP selectivity on FeP/TiO_2 catalysts (C) Pyrazine selectivity on FeP/TiO_2 catalysts at 653 K.

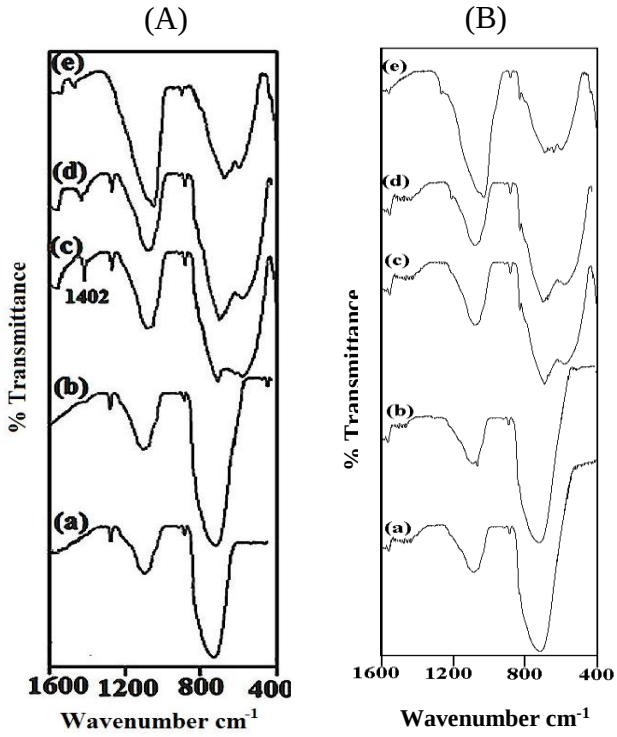

Fig. 5. FTIR spectra of (A) spent and (B) fresh FeP/TiO_2 catalysts. (a) 5FeP/TiO_2; (b) 10FeP/TiO_2; (c) 15FeP/TiO_2; (d) 20FeP/TiO_2; (e) 25FeP/ TiO_2.

Table-2. Catalytic activity results obtained at 653 K with 2-MP/water/ammonia/air ratio = 1/13/ 17/38.

Catalyst	% Conversion 2-MP	% Yield 2-CP	Reference
Pure TiO_2	25	16.5	Present study
15FeP/CeO_2	59	44	Present study
15FeP/ZrO_2	80	48	Present study
15FeP/TiO_2	75.5	69	Present study
Bulk $FePO_4$	45	43	[19]
15AMPV/SiO_2	66	40	[26]
Bulk 3Mo/$FePO_4$	70	63	[27]

AMPV= vanadium incorporated ammonium salt of molybdophosphoric acid

On the other hand, at higher FeP loadings (20 and 25 wt%) aggregation of $FePO_4$ and titanium phosphate formation decreased the catalytic activity. Hence, to obtain the maximum 2-CP yield of 69% at least 15 wt% of FeP loading was necessary on TiO_2. FTIR analysis of spent 15FeP/TiO_2 showed facile ironammonium complex formation at higher acidity.

Acknowledgement: *This work was supported by the Chemical and Materials Engineering Department at King Abdulaziz University, Jeddah, Saudi Arabia.*

REFERENCES

1. G. Ertl, H. Knozinger, J. Weitkamp, in: Handbook of Heterogeneous Catalysis, vol. 5, Wiley-VCH, 1997, p. 2322.
2. B. Lucke, A. Martin, in: Fine Chemicals through Heterogeneous Catalysis, R. Sheldon, H. van Bekkum (eds.), Wiley-VCH, Weinheim, 2001, p. 527.
3. Ger. Pat. 1940320 (1972).
4. G. C. Bond, P. Konig, *J. Catal.*, **77,** 309 (1982).
5. I. E. Wachs, R.Y. Saleh, S. S. Chart, C. C. Chersich, *Appl. Catal.*, **15,** 339 (1985).
6. F. Cavani, E. Foresti, F. Trifiro, G. Busca, *J. Catal.*, **106,** 251 (1987).
7. V. M Bondareva, T. V Andrushkevich, O. B Lapina, *Catal. Today*, **61,** 173 (2000).
8. K. V. R. Chary, K. Rajender Reddy, Ch. Praveen Kumar, D. Naresh, V. Venkat Rao, G. Mestl, *J. Mol. Catal. A.*, **223,** 363 (2004)
9. K. V. R. Chary, K. Rajender Reddy, Ch. Praveen Kumar, *Catal. Commun.*, **2,** 277 (2001).
10. K. V. Narayana, A. Martin, *Catal. Today*, **157,** 275 (2010).
11. D. Naresh, K. V. Narayana Kalevaru, A. Martin, *Catalysts*, **10,** 1 (2016).
12. P. Nagaraju, N. Lingaiah, M. Balaraju, P. S. Sai Prasad, *Appl. Catal. A: Gen.*, **339,** 99 (2008).
13. P. Nagaraju, Ch. Srilakshmi, N. Pasha, N. Lingaiah, I. Suryanarayana, P. S. Sai Prasad, *Catal. Today*, **131,** 393 (2008).
14. R. L. McCormick, G. O. Alptekin, *Catal. Today*, **55,** 269 (2000).
15. P. Villabrille, P. Vazquez, M. Blanco, C. Caceres, *J. Colloid. Interface.*, **251,** 151 (2002).
16. X. Wang, Y. Wang, Q. Tang, Q. Guo, *J. Catal.*, **217,** 457 (2003).
17. M. Ai, E. Muneyama, A. Kunishige, K. Ohdan, *J. Catal.*, **144,** 632 (1993).
18. R. Glaum, M. Reehuis, N. Stuber, U. Kaiser, F. Reinauer, *J. Sol. Chem.*, **126,** 15 (1996).
19. P. Nagaraju, Ch. Srilakshmi, Nayeem Pasha, N. Lingaiah, I. Suryanarayana, P. S. Sai Prasad, *Appl. Catal. A.*, **334,** 10 (2008).
20. K. Mallick, M. J. Witcomb, M. S. Scurrell, *Appl. Catal. A.*, **259** 163 (2004).
21. S. del Val, M. L. Granados, J. L. G. Fierro, J. S. Gonzalez, A. J. Lopez, *J. Catal.*, **188,** 203 (1999).
22. K. Schwarzer, A. Hausweiler, US3280167A (1966).
23. S. X. Liu, X. Y. Chen, X. Chen, *J. Hazard. Mat.*, **143,** 257 (2007)
24. Ch. Pan, S. Yuan, W. Zhang, *Appl. Catal. A.*, **312,** 186 (2006).
25. A. Martin, Y. Zhang, H. W. Zanthoff, M. Meisel, M. Baerns, *Appl. Catal. A.*, **139,** L11 (1996).
26. K. Mohan Reddy, N. Lingaiah, P. Nagaraju, P. S. Sai Prasad, *Catal. Lett.*, **122,** 314 (2008).
27. P. Nagaraju, H. Driss, Y. A. Alhamed, A. A. Alzahrani, M. A Daous, L. Petrov, N. Lingaiah, P. S. Sai Prasad, *J. Chem. Sci.*, **128,** 227 (2016).
28. D. A. Panayotov, J. R. Morris, *J. Phys. Chem. C.*, **113,** 15684 (2009).